

# Supporting Information

## Elucidating Anionic Redox Chemistry in P3-layered Cathode for Na-ion Batteries

*Min Jia,<sup>†,‡</sup> Haifeng Li,<sup>&</sup> Yu Qiao<sup>\*,†</sup>, Linlin Wang,<sup>§</sup> Xin Cao,<sup>†,‡</sup> Jordi Cabana<sup>&</sup> and Haoshen Zhou<sup>\*,†,‡,§</sup>*

<sup>†</sup>Energy Technology Research Institute, National Institute of Advanced Industrial Science and Technology (AIST), 1-1-1, Umezono, Tsukuba 305-8568, Japan. E-mail: kyou.qiaoyu09206@aist.go.jp (Y. Q.) E-mail: hs.zhou@aist.go.jp (H. Z.).

<sup>&</sup> Department of Chemistry, University of Illinois at Chicago, Chicago, Illinois 60607, United States

<sup>§</sup>Center of Energy Storage Materials & Technology, College of Engineering and Applied Sciences, Jiangsu Key Laboratory of Artificial Functional Materials, National Laboratory of Solid State Microstructures, and Collaborative Innovation Center of Advanced Microstructures, Nanjing University, Nanjing 210093, P. R. China  
E-mail: hszhou@nju.edu.cn (H. Z.)

<sup>‡</sup>Graduate School of System and Information Engineering, University of Tsukuba, 1-1-1, Tennoudai, Tsukuba 305-8573, Japan

<sup>§</sup>Nanjing Univ, Sch Chem & Chem Engr, Collaborat Innovat Ctr Chem Life Sci, State Key Lab Analyt Chem Life Sci, Nanjing 210093, Jiangsu, P. R. China

## Experimental Section

### Synthesis of $\text{Na}_{0.5}\text{Mg}_{0.15}\text{Al}_{0.2}\text{Mn}_{0.65}\text{O}_2$ (NMAMO) material:

$\text{Na}_{0.5}\text{Mg}_{0.15}\text{Al}_{0.2}\text{Mn}_{0.65}\text{O}_2$  sample was synthesized by solid state reaction from stoichiometric amounts of  $\text{Na}_2\text{CO}_3$ ,  $\text{MgO}$ ,  $\text{Al}_2\text{O}_3$  and  $\text{MnO}_2$ , and amount of  $\text{Na}_2\text{CO}_3$  was added with 5 wt% excess. The starting stoichiometric mixture was ground together and then held at 700 °C for 24 h under air atmosphere. The resulting black powder was reground and carefully checked for impurity phases using x-ray diffraction.

### Materials Characterizations:

The structure of  $\text{Na}_{0.5}\text{Mg}_{0.15}\text{Al}_{0.2}\text{Mn}_{0.65}\text{O}_2$  material was identified by powder XRD (Ultima III, Rigaku Corporation) radiation from Cu  $K\alpha$  ( $\lambda = 1.5406 \text{ \AA}$ ). The data were collected between diffraction angles ( $2\theta$ ) from  $10^\circ$  to  $80^\circ$  at a scan rate of  $2^\circ$  per min. Rietveld refinements of the XRD pattern obtained by GSAS + EXPGUI suite. In-situ Raman spectra of the materials were obtained using a homemade mould and JASCO microscope spectrometer (NRS-1000DT). In-situ DEMS measurements were carried out using a homemade cell connected to the equipment from Perkin-Elmer (Clarus 680 and SQ 8S). XPS was characterized by a Thermo Fisher Scientific Model  $K\alpha$  spectrometer equipped with Al  $K\alpha$  radiation (1486.6 eV). The composition of the material was confirmed by inductively coupled plasma (ICP), (M90, Bruker), HRTEM image were taken with a JEM-200c transmission electron microscope operated at 200 kV.

### Electrochemical tests:

2032 coin-type cells were used for electrochemical measurements. The electrodes consisted of active material, acetylene black, and polytetrafluoroethene (PTFE, 12 wt.%) binder with the weight ratio of 80:10:10. The mass loading of the active material in the electrode is around  $2.2 \sim 2.6 \text{ mg cm}^{-2}$ . 1 M  $\text{NaClO}_4$  in propylene carbonate (PC) was

prepared as the electrolyte. Battery tester system HJ1001 SD8 (Hokuto Denko) were employed for galvanostatic testing.

### **X-ray Absorption Spectroscopy**

*Ex situ* O K-edge X-ray absorption spectroscopy (XAS) measurements were performed at 4-ID-C beamline of APS at Argonne National Laboratory. Samples were attached to a copper sample holder using conductive carbon tape in an argon-filled glovebox and then transferred from the glovebox into a transport container and then into an X-ray absorption antechamber through an argon environment to minimize the potential exposure to air. Data were measured simultaneously under both the total electron yield (TEY) mode from the sample photocurrent at  $\sim 10^{-9}$  Torr and total fluorescence yield (TFY) mode using a silicon drift diode detector. The angle of X-ray incidence in TFY mode was adjusted to minimize the self-absorption while still being bulk sensitive. Data was obtained at a spectral resolution of  $\sim 0.2$  eV, with a 2 s dwell time. During the measurement, three scans were performed at each absorption edge for each sample, and scans were then averaged to maximize the signal-to-noise ratio. The energy scale of the spectra was calibrated with a  $\text{Sr}_2\text{RuO}_4$  reference measured simultaneously.

### **In-situ Raman observation**

A detailed description of the modified in-situ Raman cell (Hohsen Corp., Osaka, Japan) for the Na-ion battery was employed. In detail, a thin quartz window (thickness, 0.5 mm) has been fixed on the top of the cell as a sight window. In order to collect shell-isolated nanoparticle-enhanced Raman (SHINER) signal, gold nanoparticles (NPs) approximately 40 nm in diameter with a  $\text{SiO}_2$  coating shell ( $\sim 5$  nm) were synthesized. The washed and dried  $\text{Au}@\text{SiO}_2$  NPs were dripped onto the specific cathode surface and vacuum dried before

assembly. The cathode was assembled at the bottom of the cell with the active material-face upward. On the top of the cathode, 50  $\mu\text{L}$  of electrolyte (1 M  $\text{NaClO}_4$  in propylene carbonate (PC) ) was homogeneously dropped onto the glassy fiber filter separator (GF/A, Whatman). As a standard two-electrode configuration cell, lithium foil (thickness, 0.4 mm) was assembled at the top as the reference and counter electrode. Note that, a small hole was punched on the center of both the separator and Na metal, through which the laser and Raman signals can fluidly cross. The cell was assembled in an argon-filled glovebox. Besides, bulk-sensitive Raman measurements use the same in-situ Raman cell (Hohsen Corp., Osaka, Japan) with same cell assembling conditions.

The Raman spectra were recorded using a JASCO microscope spectrometer (NRS-1000DT). The excitation light of an air-cooled He–Ne laser at 632.8 nm wavelength was focused on the electrode surface through a 50 $\times$ long working distance lens (Olympus America Inc.). The confocal slit was adjusted to be 4.0  $\mu\text{m}$  to minimize the band broadening effect due to the contribution of non-confocal signal. The scattered light was collected in a backscattering geometry along the same optical path as the pumping laser. The power of laser beam delivered to the electrode surface was roughly 10% of the maximum 30 mW laser intensity, unless specified, to avoid degradation to the products and/or cathode in SHINER while the estimated power on the sample was 0.43 mW in bulk-sensitive Raman. The Raman spectrum acquisition time varied from 600~800 s with 2 accumulations. At least 3 different places on the electrode surface at each cathode plate were checked to ensure the Raman spectra were credible and reproducible. The spectral resolution of the Raman spectra in the study was ca. 1.0  $\text{cm}^{-1}$ .

For the in-situ Raman test, the electrochemical experiments were carried out under the control of a potentiostat (Potentiostat/Galvanostat PGSTAT30, Autolab Co. Ltd., Netherlands) at room temperature. The current and potential outputs from the potentiostat were recorded by a multifunction data acquisition module/amplifier (PGSTAT30 Differential

Electrometer, Autolab), which was controlled by General Purpose Electrochemical Software (GPES). Typically, the galvanostatic control was carried out at a current density of 20 mA g<sup>-1</sup>. Before characterization, the cell was kept on an open circuit for 10 h. The OCV was approximately 2.8 V in most cases in the study. All the potentials in this study were referenced to Na/Na<sup>+</sup>.

#### **In-situ Differential Electrochemical Mass Spectrometry (DEMS) measurements:**

In situ Differential Electrochemical Mass Spectrometry (DEMS) measurements were carried out using a homemade cell connected to the equipment from Perkin-Elmer (Clarus 680 and SQ 8S). The mass spectrometer absolute sensitivity is calibrated for CO<sub>2</sub> and O<sub>2</sub>, therefore, the evolution rate of these gases can be obtained.

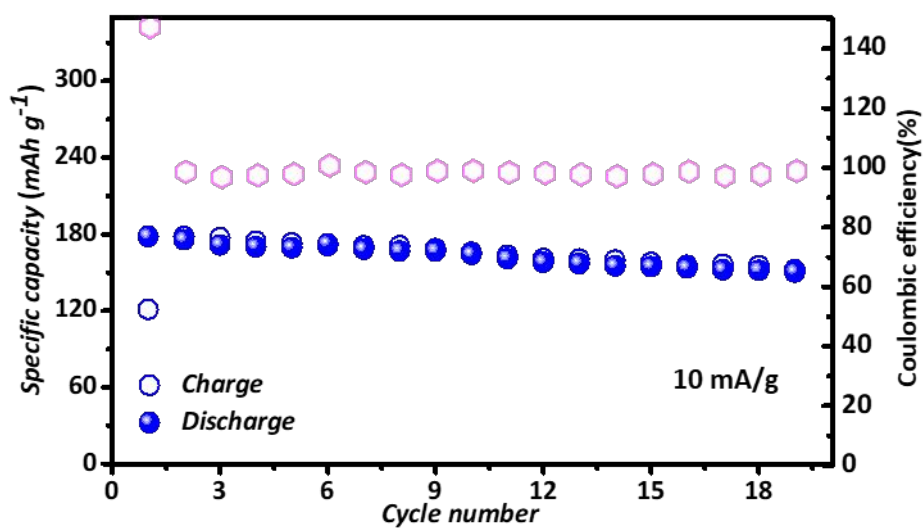


**Figure S1.** The cycling performance of NMAMO at current density of 10 mA g<sup>-1</sup>.

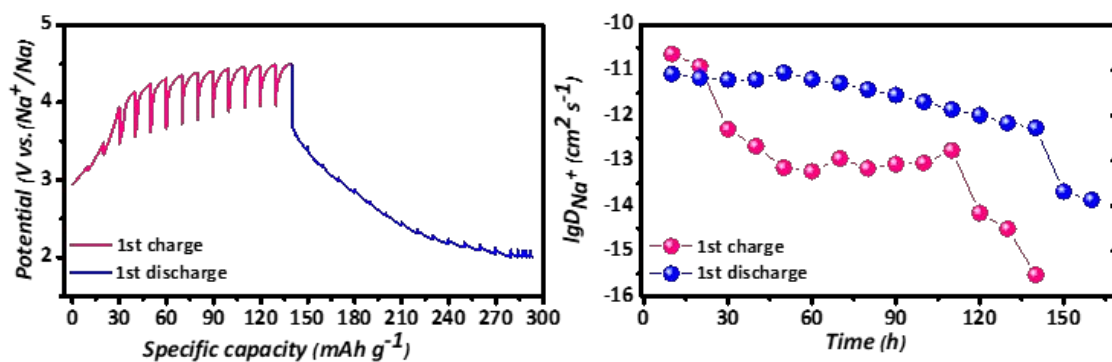


**Figure S2.** GITT results of P3-NMAMO cathode for the first cycle with the variation of quasi-equilibrium potentials and the calculated Na<sup>+</sup> diffusion coefficient.

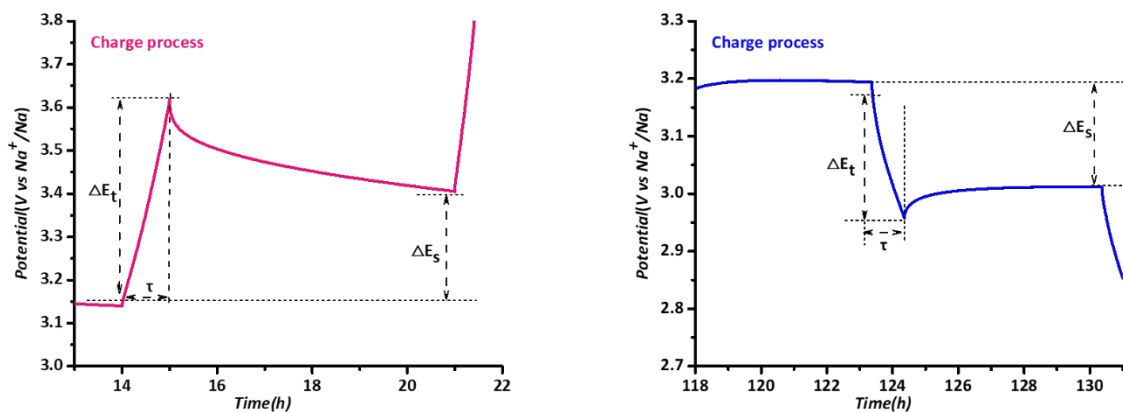


**Figure S3.** The potential profile for a single titration at 3.15 V during charge process with labelling the different parameters (left). The potential profile for a single titration at 3.18 V during discharge process with labelling the different parameters (right). The simplifying equation of Fick's second law to calculate diffusion coefficient ( $D/R^2$ ), where  $\tau$  is the limited time period,  $nm$  is the mole number of the electrode,  $V_m$  is the molar volume of the NMAMO,  $S$  is the area of electrode,  $\Delta E_s$  and  $\Delta E_t$  are the change in the steady state potential and the total change during the current flux by deducting the IR drop, respectively.

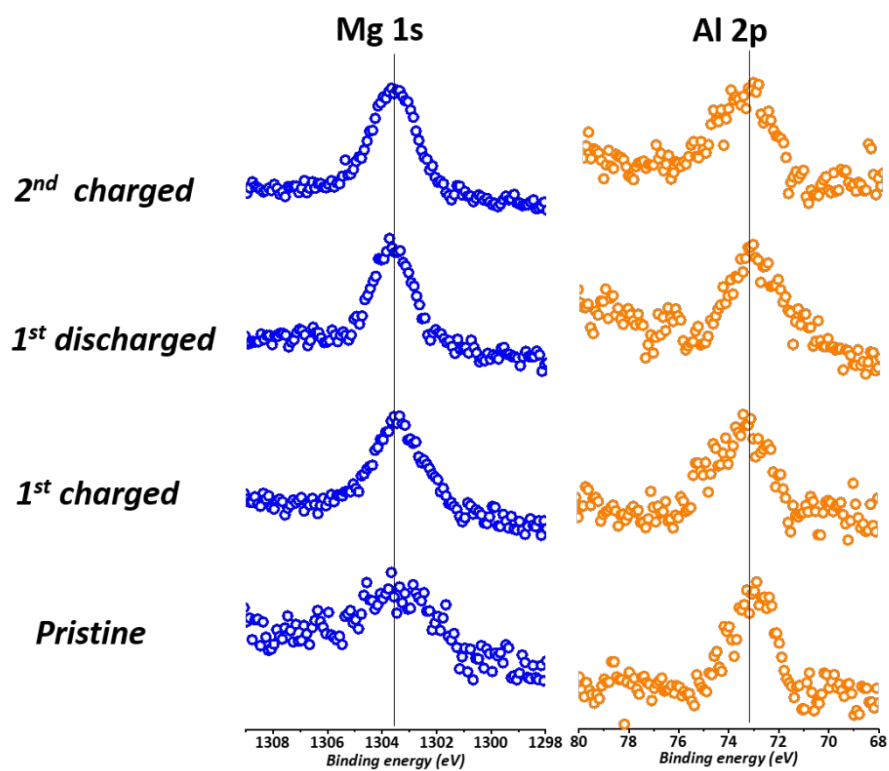


**Figure S4.** Mg 1s and Al 2p spectrum of NMAMO cathode.

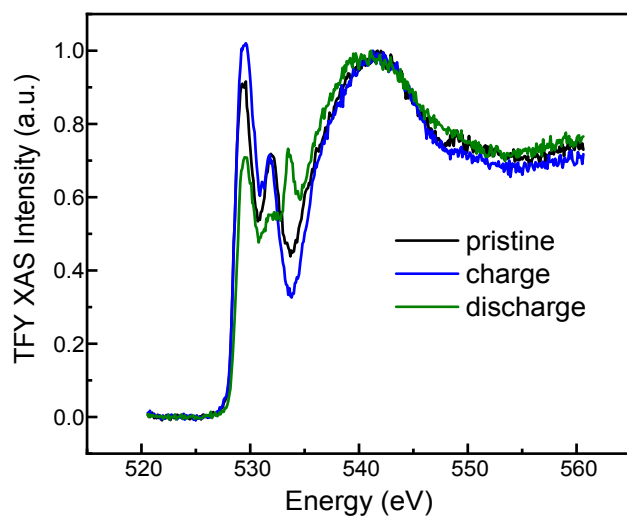


**Figure S5.** *Ex situ* O K-edge XAS spectra of NMAMO electrode at different states of charge.

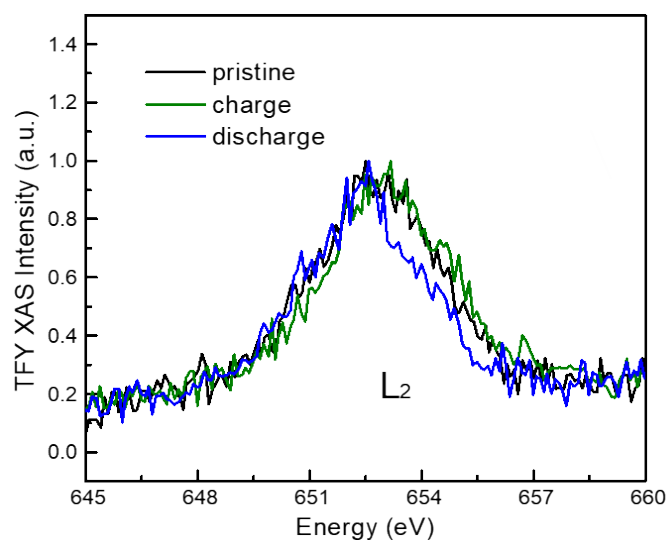


**Figure S6.** *Ex situ* Mn L-edge XAS spectra of NMAMO electrode at different states of charge. For L<sub>2</sub>-edge, the peak position remained constant upon charge and shifted to lower energy in the subsequent discharge, suggesting the preservation of Mn<sup>4+</sup> upon charge and the reduction of Mn upon discharge.

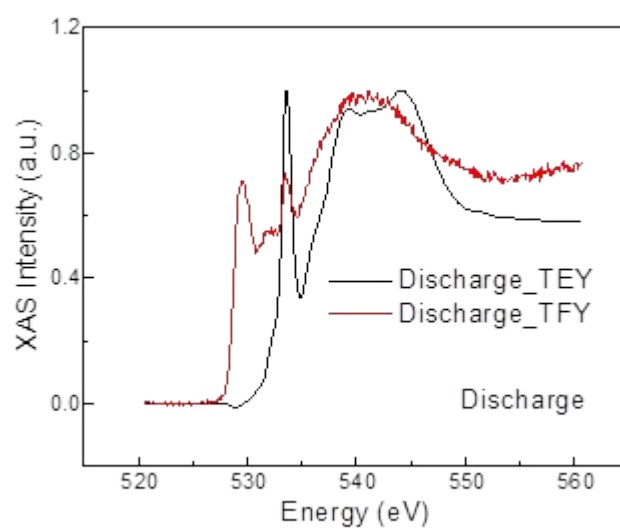


**Figure S7.** *Ex situ* O K-edge XAS spectra of NMAMO electrode after fully discharged to 2 V.

**Table S1.** Refinement crystallographic parameters by Rietveld analysis for NMAMO. S.G. R

3m a = b = 2.86, c = 16.87,  $\alpha = \beta = 90^\circ$   $\gamma = 120^\circ$ , Rwp = 6.38%,  $\chi^2 = 3.145$ .

Atom	site	x	y	z	Occ.
Na1	3a	0	0	0.836	0.5
Mg1	3a	0	0	0	0.15
Al1	3a	0	0	0	0.2
Mn1	3a	0	0	0	0.65
O1	3a	0	0	0.382	1
O2	3a	0	0	0.618	1

**Table S2.** Stoichiometry from ICP analysis of the  $\text{Na}_{0.5}\text{Mg}_{0.15}\text{Al}_{0.2}\text{Mn}_{0.65}\text{O}_2$  material.

		Na	Mg	Al	Mn
$\text{Na}_{0.5}\text{Mg}_{0.15}\text{Al}_{0.2}\text{Mn}_{0.65}\text{O}_2$	Conc.(mg/L)	1.141	0.367	0.553	3.687
	Stoichiometric ratio	0.4961	0.1529	0.2048	0.6703

**Table S3.** Refinement crystallographic parameters by Rietveld analysis for NMAMO cathode after 100 cycles.

<i>Space group</i>	<b>R 3m</b>	
<i>Cell parameters</i>	<i>a</i>	2.88
	<i>b</i>	2.88
	<i>c</i>	17.07
	<i>a</i>	90 °
	<i>β</i>	90 °
	<i>γ</i>	120 °
<i>Agreement factors</i>	<i>Rwp%</i>	7.75
	<i>Rp%</i>	5.69
	<i>χ<sup>2</sup></i>	5.065

**Table S4.** Refinement crystallographic parameters by Rietveld analysis for NMAMO aging for 3 months.

<i>Space group</i>	<b>R 3m</b>	
<i>Cell parameters</i>	<i>a</i>	2.83
	<i>b</i>	2.83
	<i>c</i>	16.70
	<i>a</i>	90 °
	<i>β</i>	90 °
	<i>γ</i>	120 °
<i>Agreement factors</i>	<i>Rwp%</i>	5.48
	<i>Rp%</i>	4.43
	<i>χ<sup>2</sup></i>	2.183